Clinical Cancer Research

Coadministration of Trametinib and Palbociclib Radiosensitizes KRAS-Mutant Non–Small Cell Lung Cancers *In Vitro* and *In Vivo*

Zhen Tao[1,2], Justin M. Le Blanc[1], Chenguang Wang[3], Tingting Zhan[4], Hongqing Zhuang[2], Ping Wang[2], Zhiyong Yuan[2], and Bo Lu[1]

Abstract

Purpose: To investigate the potential roles that p16 (CDKN2A) and RB activation have in sensitization to MEK inhibitor in resistant KRAS-mutant non–small cell lung cancer cells (NSCLC) *in vitro* and *in vivo*.

Experimental Design: Cell viability was measured with MTS assays. Effects of administration of radiation and combination drug treatments were evaluated by clonogenic assay, flow cytometry, and Western blots. DNA repair was assessed using immunofluorescent analysis. Finally, lung cancer xenografts were used to examine *in vivo* effects of drug treatment and radiation therapy.

Results: In this study, we showed that sensitivity to MEK inhibitor correlated to the RB/p16/CDK4 pathway and knockdown of RB induced resistance in cell lines sensitive to MEK inhibitor. Also, overexpression of p16 and inhibition of CDK4 had the ability to sensitize normally resistant cell lines. Our data indicated that the MEK inhibitor (trametinib, GSK112012) cooperated with the CDK4/6 inhibitor (palbociclib, PD0332991) to strongly reduce cell viability of KRAS-mutant NSCLCs that were resistant to the MEK inhibitor *in vitro* and *in vivo*. In addition, we report for the first time that resistance of KRAS-mutant NSCLCs to MEK inhibitor is, at least partly, due to p16 mutation status, and we described a drug combination that efficiently reactivates the RB tumor suppressor pathway to trigger radiosensitizing effects, apoptosis, and cell-cycle arrest.

Conclusions: Our findings suggest that MEK inhibitor in combination with CDK4/6 inhibitor has significant anti-KRAS–mutant NSCLC activity and radiosensitizing effect in preclinical models, potentially providing a novel therapeutic strategy for patients with advanced KRAS-mutant NSCLCs. *Clin Cancer Res; 22(1); 122–33. ©2016 AACR.*

Introduction

Lung cancer is one of the leading causes of mortality worldwide (1). Non–small cell lung cancers (NSCLC) represent 85% of all lung cancers and generally present at advanced stages, requiring intensive multimodal therapy. Despite these medical interventions, 5-year survival rates are less than 5% (2). With the advancement in understanding about activating mutations in NSCLCs, many treatments have been developed with success against the array of different mutations identified in NSCLCs, such as EGFR, ALK, etc (3–7). The benefits that patients have seen with these treatment models have not translated well for NSCLCs harboring KRAS mutations (8–10).

Present in roughly 20% of patients with NSCLC, KRAS mutations lead to the constitutive activation of mitogen-activated protein kinase (MAPK) pathways resulting in increased levels of proliferation. This mutation leads to decreased efficacy and resistance to chemotherapeutics and radiotherapy (11–14). Previous efforts have shown the use of MEK inhibitor (MEKi) in cancer cells harboring KRAS mutations (13, 15, 16). However, pharmacologic agents targeting activated RAS proteins have been unsuccessful to date due to the development of cellular resistance.

Use of a MEKi is an attractive therapeutic option because of its limited cross-interactions (17, 19). However, no effective therapy exists for KRAS-mutant cancers, largely because KRAS itself has proven difficult to target directly with small molecules (20). Targeting single KRAS effector pathways has also failed to induce clinical responses (21) likely because KRAS activates multiple critical effectors such as the MEK/ERK, PI3K/AKT, and NF-κB pathways (22, 23). The complications seen in KRAS mutant NSCLCs responsiveness to treatments makes finding alternative pathways that sensitize KRAS cell lines to MEKi an important task.

Puyol and colleagues unveiled a synthetic lethal interaction between KRAS and cyclin-dependent kinase 4 (CDK4) in a mouse tumor model that closely mirrors NSCLCs (24). CDK4 alleles were targeted in advanced KRAS-mutant tumors, inducing apoptosis and preventing tumor progression. A recent study has also

[1]Department of Radiation Oncology, Bodine Cancer Center, Thomas Jefferson University, Philadelphia, Pennsylvania. [2]Department of Radiation Oncology, Tianjin Medical University Cancer Institute and Hospital, Tianjin, China. [3]Institute of Radiation Medicine, Chinese Academy of Medical Sciences, Peking Union Medical College, Tianjin, China. [4]Department of Pharmacology and Experimental Therapeutics, Division of Biostatistics, Thomas Jefferson University, Philadelphia, Pennsylvania.

Note: Supplementary data for this article are available at Clinical Cancer Research Online (http://clincancerres.aacrjournals.org/).

Z. Tao and J.M. Le Blanc contributed equally to this article.

Corresponding Authors: Bo Lu, Department of Radiation Oncology, Thomas Jefferson University and Hospitals, Inc., G-301 Bodine Cancer Center, 111 South 11th Street Philadelphia, PA 19107. Phone: 215-955-6705; Fax: 215-503-0013; E-mail: bo.lu@jefferson.edu; and Zhen Tao, Department of Radiation Oncology, Tianjin Medical University Cancer Institute and Hospital, Tianjin, China 300060. Phone: 86-22-23340123; Fax: 86-22-23340123; E-mail: ztao@tmu.edu.cn

doi: 10.1158/1078-0432.CCR-15-0589

Translational Relevance

Although KRAS mutations were identified in non–small cell lung cancer (NSCLC) tumors more than 20 years, 5-year survival rates remain poor, and it is resistant to chemotherapy, radiotherapy, and EGF receptor tyrosine kinase inhibitors (EGFR TKI). Thus, there is an urgent need to improve clinical outcomes. The present study identified inherent resistance of KRAS-mutant NSCLC to MEK inhibitor due to p16 mutation status. The combination of MEK inhibitor and CDK4/6 inhibitor, with the addition of radiation, could sensitize KRAS-mutant NSCLC, which led to a significant increase in cell death and a reduction in overall tumor volume. The drug combination efficiently reactivates the RB tumor suppressor pathway to trigger radiosensitizing effects, apoptosis, and cell-cycle arrest. The critical role that p16 status has in KRAS-mutant NSCLC responsiveness to MEK inhibitor shows that this could be used as a biomarker to guide treatment of these patients and improve outcomes.

shown that the mutation of KRAS can result in an increased expression of CDK4 and cyclin D1, which facilitates cell proliferation and promotes tumorigenesis (25). Therefore, this explains why targeting CDK4 may facilitate lethality in KRAS-mutant tumors, which could shed new light on treatments for KRAS-mutant NSCLCs.

Recent studies in colon cancers have shown the retinoblastoma (RB)-reactivating activity of trametinib (GSK1120212), which is an allosteric inhibitor of MEK1/2 (13, 26). CDK4/RB pathway involvement in MEKi sensitivity led us to investigate this cell-cycle regulatory pathway. The present study sought to examine the impact of RB pathway proteins on MEKi activity. We wanted to examine whether additional therapeutic strategies might improve initial response and therapeutic resistance to MEKi in KRAS-mutant NSCLCs.

Materials and Methods

Cell culture and small-molecule inhibitors

The human NSCLC cell lines A549, H23, H460, Calu-1, SK-LU-1, and H358 were purchased from the ATCC and authenticated via short tandem repeat profiling before experiments. Cells used for this study were cryopreserved within 6 months of authentication. All cells were cultured in RPMI-1640 (Invitrogen), supplemented with 10% FBS (Invitrogen) and 1% penicillin/streptomycin (Invitrogen) at 37°C in a humidified 5% CO_2 atmosphere. GSK1120212 (trametinib) was provided by GlaxoSmithKline Pharmaceutical. PD0332991 was purchased from Selleck Chemicals. A stock solution was prepared in 100% DMSO (Sigma) and stored at −20°C. The drug was diluted in fresh media prior to each experiment.

siRNA reagents and plasmid transfection

All siRNAs were obtained from Dharmacon and were used as "SMARTpools" according to the manufacturer's instructions. The day before siRNA transfection, 20×10^4 and 2,000 cells were plated in 6- and 96-well plates, respectively, and incubated in antibiotic-free medium with 10% FBS. After 24 hours, the medium was changed with antibiotic-free Opti-MEM Reduced-Serum Medium. Lipofectamine RNAiMax (Invitrogen) was used to transfect on-target siRNA or nontarget siRNA into cells. Both on-target siRNA and nontarget siRNA were used at the same concentration in all experiments. The efficiency of inhibition was determined by Western blotting after 48-hour transfection. pCMV-$p16^{INK4A}$ plasmid was purchased from Addgene and transfected using Lipofectamine 2000 (Invitrogen).

Cell viability assay

MTS assays were performed using tetrazolium-based CellTiter 96 AQueous One Solution Cell Proliferation assay (Promega). Cells were seeded in 96-well plates at 3,000 cells per well. Following adhesion of cells to the well, cells were treated with increasing concentrations of GSK1120212. Control groups were exposed to the same concentration of DMSO. MTS assay was performed at 72 hours after treatment. At 37 °C in humidified 5% CO_2, plates were read at the absorbance of 490 nm on a microplate reader (SpectraMax M5). Relative cell viability of an individual sample was calculated by normalizing their absorbance to that of the corresponding control. The combination index value was determined from the fraction affected (Fa) value of each combination according to the Chou–Talalay method by using CompuSyn software (ComboSyn, Inc.), and a combination index value below 1 represents synergism (27). All experiments were done in triplicate.

Clonogenic survival assay

Cells were grown exponentially in a 100-mm dish where they were trypsinized and counted. Cells were diluted serially to appropriate densities and plated in triplicate in 60-mm dishes. After adhesion, cells were treated with vehicle (final DMSO concentration of 0.1%; we confirmed that this DMSO concentration did not affect the proliferation of NSCLC cell lines), 10 nmol/L GSK1120212, or 1 μmol/L PD0332991 for 1 hour, then irradiated using a PanTak 310 keV X-ray machine at 0.25-mm Cu plus 1-mm Al added filtration at 125 cGy/min. After irradiation, the cells were washed with PBS and cultured in drug-free medium for 10 to 14 days. The number of colonies containing at least 50 cells was determined. After correcting for drug toxicity, plating efficiency, survival fractions, and dose enhancement ratios (DER) were calculated according to previously described methods. Experiments were repeated 3 independent times.

Western blots

Cells were washed twice with ice-cold PBS and then lysed in M-Per mammalian lysis buffer (Thermo Scientific). The protein concentration of the lysates was determined with the Bradford reagent (Bio Rad), and equal amounts of protein were subjected to SDS-PAGE. Separated proteins were transferred to a nitrocellulose membrane. This was then exposed to 5% nonfat dried milk in TBS containing 0.1% Tween-20 (0.1% TBST) for 1 hour at room temperature and then incubated overnight at 4°C with antibodies against phospho-ERK (Thr202/Tyr204), phospho-RB (Ser807/811), BIM, CDK4 (from Cell Signaling Technology), ERK, p16, RB, PARP (from Santa Cruz Biotechnology), and β-actin (Sigma-Aldrich). The membranes were then washed with 0.1% TBST before incubation with horseradish peroxidase–conjugated goat antibodies to rabbit or mouse (Santa Cruz Biotechnology). Specific bands were detected using the enhanced chemoluminescence reagent (ECL plus; Thermo Fisher Scientific) before exposing film.

Flow cytometry (FACS)

For cell-cycle analysis, cells were trypsinized, washed with cold PBS, fixed with 70% ethanol, and stored at −20°C. Fixed cells were washed with 0.5% BSA and incubated in a solution containing 0.1% Triton X-100, 0.2 mg/mL RNase A, and 25 μg/mL propidium iodide (PI). After 15 minutes of incubation at room temperature, samples were analyzed by BD LSR II cytometer (BD Biosciences). The Annexin V-FITC binding assay was performed to determine the apoptosis rate of cells *in vitro*. Briefly, cells were seeded in a 6-well plate overnight, harvested 48 hours after treatment, and incubated with 5 μL of Annexin V-FITC and 5 μL PI for 15 minutes at room temperature in the dark. Cells were analyzed using BD LSR II cytometer (BD Biosciences). Each experiment was performed 3 times. Data were analyzed using FlowJo software (Tree Star, Inc.).

Immunofluorescent analysis of γH2AX foci

Cells grown in chamber slides, were fixed in 2% paraformaldehyde for 15 minutes at room temperature, and permeabilized with 1% Triton X-100 for 10 minutes on ice.

Slides were incubated in anti-phospho γH2AX (Millipore) overnight, an Alexa Fluor 594 Donkey Anti-Mouse secondary antibody (Invitrogen) for 1 hour at room temperature and mounted with ProLongGold Antifade Reagent with DAPI (Invitrogen) to visualize nuclei. Cells were analyzed on a Leica upright fluorescent microscope. The percentage of cells containing more than 50 foci was determined in 150 cells for each condition. Experiments were carried out in triplicate.

Animals and tumor xenograft assay

Five- to 6-week-old female athymic nude mice were obtained from Taconic Farms. Mice were caged in groups of 5, kept on a 12-hour light/dark cycle, and provided with sterilized food and water *ad libitum*. Animals were allowed to acclimate for at least 7 days before any handling. Exponentially growing A549 cells were trypsinized and washed with PBS and diluted into 2×10^6 cells per 100 μL PBS. The cell suspension was injected subcutaneously into the right flank of mice. Tumors were grown until the average tumor volume reached approximately 100 mm^3. Mice were randomized into the vehicle group, GSK1120212 only group, PD0332991 only group, irradiation only group, GSK1120212 combined with PD0332991 group, GSK1120212 combined with irradiation group, PD0332991 combined with irradiation group, and GSK1120212 combined with PD0332991 and irradiation. Each treatment group contained 8 mice. GSK1120212 was dissolved in sterile 100% DMSO and diluted 1:9 in sterile-filtered 1% carboxymethylcellulose and 0.4% Tween-80 (Sigma). The solution was then administered orally at doses of 3 mg/kg for 7 consecutive days. PD-0332991 was dissolved in sterile-filtered sodium lactate buffer (50 mmol/L, pH 4.0) and delivered by oral gavage as previously described (28). Tumors were irradiated with a fractionated schedule of 2 Gy daily over 5 consecutive days using a PanTak 310keV X-ray machine at 0.25-mm Cu plus 1-mm Al added filtration at 125cGy/min. Tumors were measured 2 to 3 times weekly using a Vernier caliper and calculated by the formula: volume (V) = length (a) × width (b) × width (b) × 0.52. Body weights were measured using an electronic scale.

Immunohistochemistry

Formalin-fixed, paraffin-embedded tumor sections were stained with cleaved caspase-3, phospho-ERK (Cell Signaling Technologies), and Ki-67 (DAKO). The bound antibodies were detected with horseradish peroxidase (HRP)-conjugated secondary antibodies and 3,3′-diaminobenzidine (DAB), which was conducted in the Thomas Jefferson University Pathology Core laboratory (Philadelphia, PA) using standard protocols. The number of positive cells per ×400 field were scored and graphed by averaging 3 repeated assessments.

Analysis of The Cancer Genome Atlas dataset

A normalized mRNA expression dataset in The Cancer Genome Atlas (TCGA) Lung Adenocarcinoma (29) was downloaded from the cBioPortal for cancer genomics and used to evaluate coexpression and overall survival of KRAS- and P16-mutant transcript levels. This dataset includes mRNA profiles for 230 lung adenocarcinoma tumor samples. Spearman correlation coefficiency was calculated for these transcripts for all primary tumor samples. Differences were considered significant with $P < 0.05$.

Statistical analyses

Data are shown as the mean ± SD. The Student t test was used to determine the significance between groups. Significance was defined at the level of $P < 0.05$. The combination index value was determined from the Fa value of each combination according to the Chou–Talalay method by using CompuSyn software (ComboSyn, Inc.; ref. 30).

Results

MEK inhibitor decreases cellular proliferation and activates p16 and RB

We first evaluated the sensitivity of MEK inhibitor (MEKi) on cell viability when used in a panel of different KRAS-mutant NSCLCs with ranging drug sensitivities. Cells received varying concentrations of MEKi (0–1,000 nmol/L) at 4 different time points (24, 48, 72, and 96 hours). MTS assays were performed on separate cell lines (Fig. 1A and Supplementary Fig. S2A), where they exhibited sensitivity to the MEKi in a time- and dose-dependent manner. All 3 cell lines had decreased survival rates; however, there was a differential in sensitivity to MEKi-induced effects. The sensitive cell line (H358) exhibited the greatest overall decrease in survival rates, whereas the more resistant cell lines (A549 and H460) had less of a response to increasing concentrations of MEKi. One interesting finding of MEKi administration was that the level of pERK was decreased within 15 minutes and almost abrogated at 30 minutes with a concentration of 10 nmol/L MEKi. (Supplementary Fig. S1A). This indicates that differential antiproliferative activity is due to differences in the intrinsic cellular nature rather than the inhibition of pERK by MEKi.

To determine whether or not the decrease in cell survival was due to apoptosis and cell-cycle arrest, we performed a cell-cycle analysis and a Western blotting to examine the cleaved PARP levels. We found that both cell-cycle arrest (Fig. 1B) and cellular apoptosis (Fig. 1C) were present with MEKi in a dose-dependent manner. We found a markedly increased percentage of cells arrested in G_1–G_0 phase in the H358 (30% increase G_1–G_0 phase MEK inhibitor vs. control, $P < 0.05$). Western blot analyses were performed on the 3 cell lines to observe the effects of MEKi on the expression levels of key cell-cycle regulatory proteins. MEKi activated RB (reduction of pRB) and induced expression of p16 in the H358 cell line, compared with no effect in the A549 and H460 cell lines (Fig. 1C).

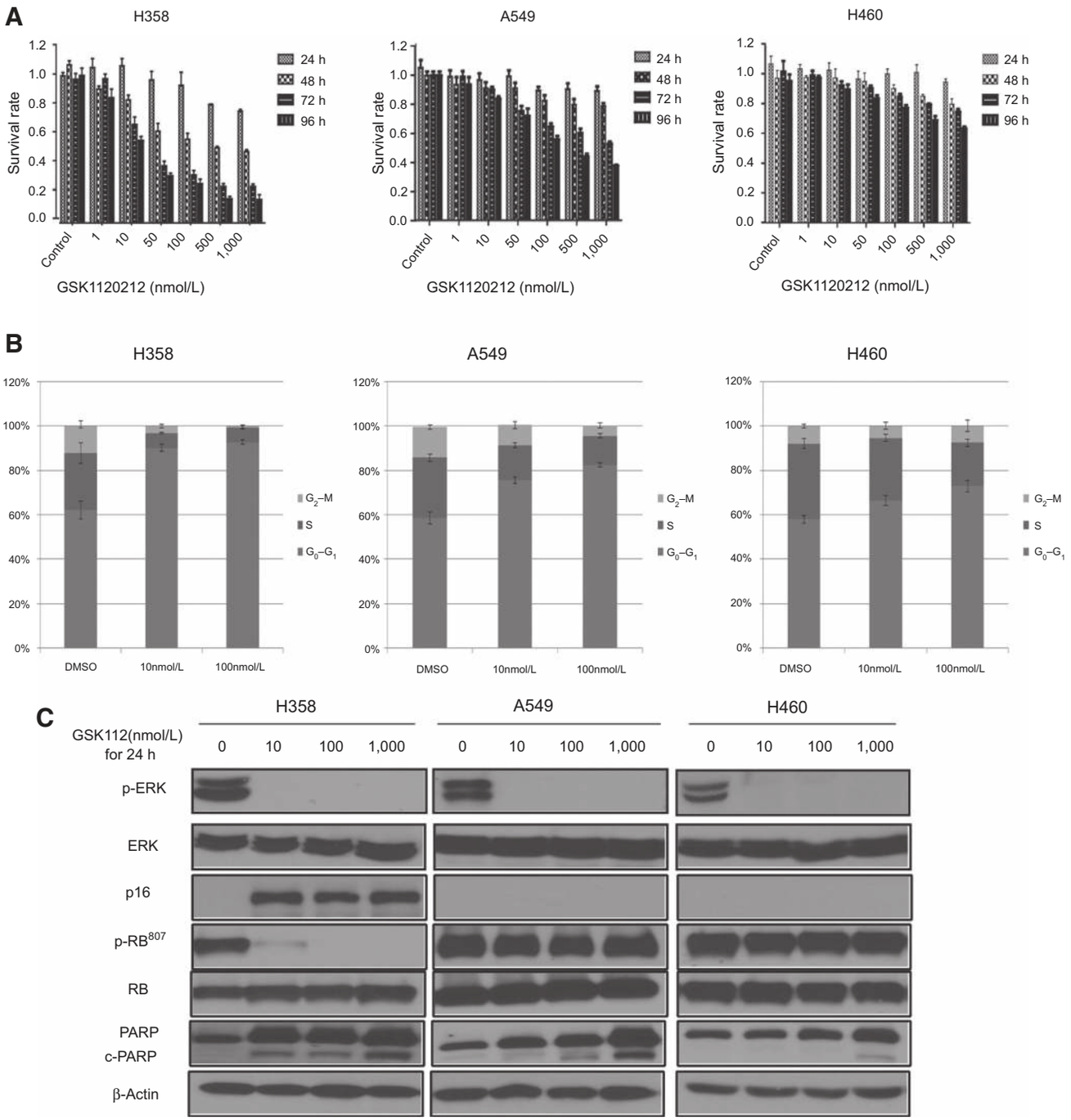

Figure 1.
Effects of MEK inhibitor (GSK1120212) on cell viability, cell cycle, and epigenetic markers. A, MTS assays were performed on 3 cell lines H358, A549, and H460 with increasing concentration of MEK inhibitor (trametinib) at 2 separate time points, 72 and 96 hours. Data are the mean ± SD of triplicate determinations. B, cell-cycle analysis was performed to quantify the distribution of cell-cycle progression. The treatment with trametinib for 24 hours dose dependently increased the G_1 phase with a decrease in the S-phase. C, Western blot analyses were performed on the 3 cell lines to analyze the administration of increasing concentration of MEK inhibitor (0–1,000 nmol/L) on the levels of apoptosis and key cell-cycle regulatory proteins.

p16/CDK4/RB regulatory protein status determines cellular sensitivity to MEK inhibitor

Cellular database information was obtained indicating the deletion of CDKN2A (i.e., p16 or INK4a) in MEKi-resistant cell lines (Supplementary Fig. S2B). By performing a search in TCGA, we determined that this deletion has a negative impact on overall cell survival when compared with the wild-type p16 status. The Kaplan–Meier analysis was conducted to evaluate the difference

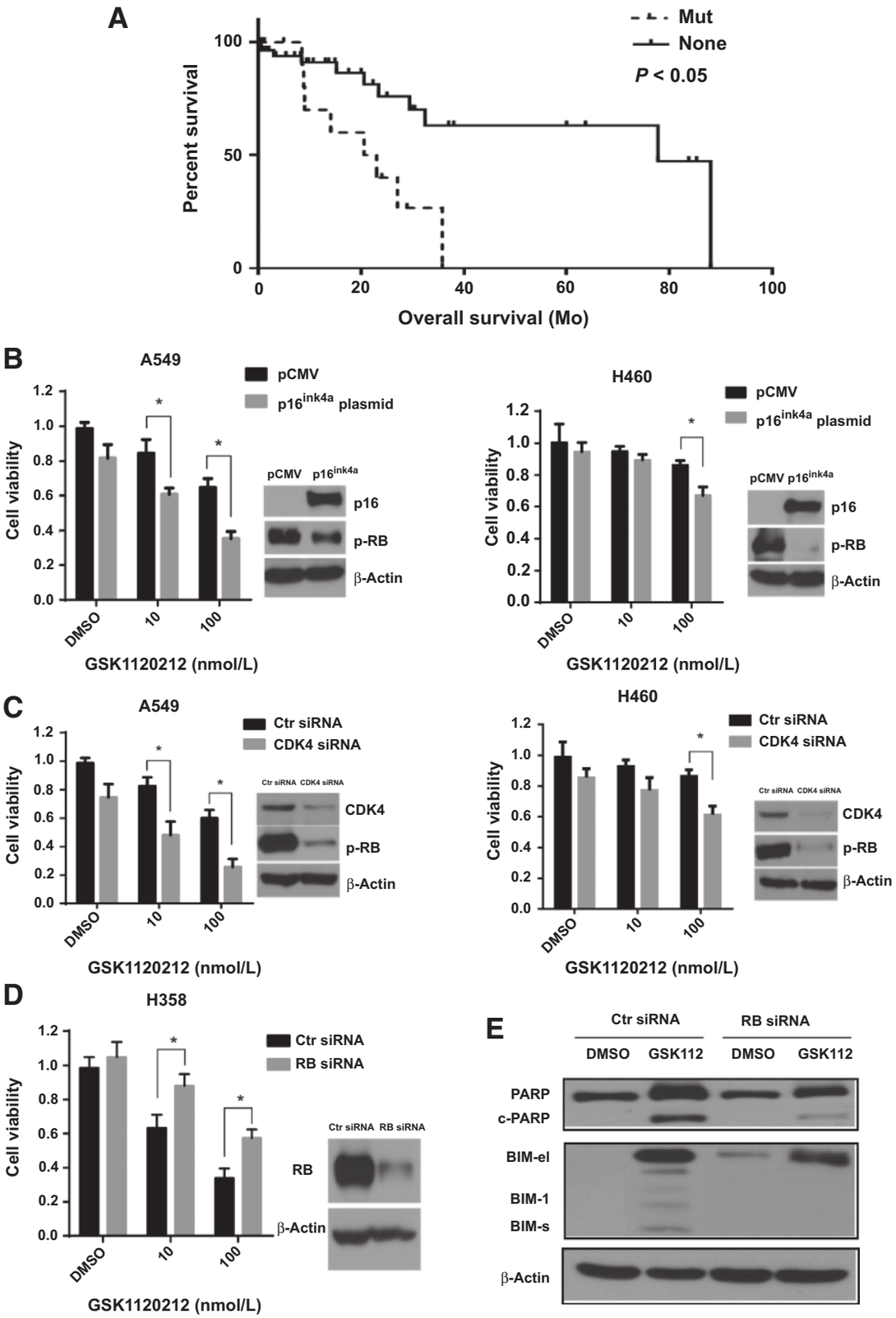

in overall survival of patients with lung adenocarcinoma ($n = 230$), among which 79 cases harbor KRAS mutation. In this cohort, 16 patients have p16 mutation and the other 63 are of wild-type. We found that patients of KRAS-mutant NSCLC who harbor wild-type p16 status had significant higher overall survival than those with p16 mutation ($P < 0.05$; Fig. 2A). To determine whether the sensitivity of MEKi was dependent upon p16 status, we performed overexpression experiments with p16 plamids on the resistant cell lines (i.e., A549 and H460), which do not express an active p16. We found that presence of a functional p16, when exposed to increasing concentrations of MEKi, could sensitize the normally resistant cell lines A549 and H460 to MEKi (Fig. 2B). Western blot analyses demonstrated that a functional p16 correlated to a reduction of pRB in A549 and H460 cell lines.

Because CDK4 is the downstream of p16 (31) and the resistant cell lines (A549 and H460) have a deficient p16 status, we performed knockdown experiments with siRNA against CDK4. An MTS assay was performed to observe the effects CDK4 knockdown had in this p16-deficient cell line. Both on-target siRNA and nontarget siRNA were used at the same concentration in all experiments. The efficiency of inhibition was determined by Western blot 48 hours after transfection. We observed a decrease in cell survival with increasing concentration of MEKi (0–100 nmol/L) when CDK4 siRNA was used (Fig. 2C) and that increasing concentrations of MEKi could sensitize the resistant cell lines. In A549 cell line, treatment with 10 and 100 nmol/L MEKi and siRNA against CDK4 reduced cell viability by about 30% compared with MEKi alone (Fig. 2C). While in H460 cell line, we found no synergism in treatment with 10 nmol/L MEKi and siRNA CDK4, but 20% reduction in cell viability by treatment of 100 nmol/L MEKi and knockdown of CDK4 compared with MEKi alone (Fig. 2C; $P < 0.05$), which might be an off-target effect.

To determine the role of RB in mediating MEKi effects, we performed MTS assays after knockdown of RB in the sensitive cell line. MTS assays demonstrated the introduction of resistance into the sensitive cell line (H358) when RB was knocked down. RB depletion in H358 cells restored cell proliferation in the presence of MEKi (Fig. 2D), suggesting that RB inactivation partly renders cells insensitive to the MEKi. Following RB knockdown, H358 cells treated with MEKi showed decreased levels of cleaved PARP as shown by Western blot analyses (Fig. 2E), compared with cells that were treated with control siRNA and MEKi. This indicated less induction of apoptosis in these cells.

MEK inhibitor and CDK4/6 inhibitor coadministration leads to cell-cycle arrest and decreases proliferation through a synergistic interaction

Because CDK4 knockdown showed an ability to sensitize the resistant cell lines (A549 and H460) to MEKi, we next introduced a pharmacologic CDK4/6 inhibitor (CDKi). To test whether targeting of CDK4 sensitizes NSCLC cells to MEK inhibitor, NSCLC cells were treated with GSK1120212, PD0332991, and their combination with different concentration for 72 hours, cell viability was measured using MTS assay. A synergistic effect was observed when GSK1120212 was combined with PD0332991 at doses that had comparatively minor effects in the single-agent treatments (Fig. 3A and Supplementary Fig. S2A). The combination index (CI) values and the Fa for each dose were used to generate the Fa–CI plots by CompuSyn software. CI < 1 represents synergism (Fig. 3B). Isobologram analysis also indicated a strong synergism of GSK1120212 with PD0332991 (Supplementary Fig. S4).

Because the RB protein plays a critical role in cell-cycle progression (32), we examined the cell-cycle effects that CDK4 inhibition has on resistant cell lines. A cell-cycle analysis was performed on the 2 resistant cell lines (Fig. 3C) to observe the impact that coadministration of the CDKi and MEKi exerts on the previously resistant cell lines. Compared with either drug alone, the combination treatment led to increased rates of G_1 arrest and a dramatic decrease in S-phase in both cell lines. MEKi alone led to a 10% to 15% increase in G_1 arrest (Fig. 1B) compared with 30% ($P < 0.05$) increase in the combination drug treatment (Fig. 3C). Taken together, our results indicate that coadministration with MEKi and CDKi synergistically increased cytotoxicity and leads to cell-cycle arrest.

MEK inhibitor enhances radiosensitivity of KRAS-mutant NSCLC cell lines leading to increased cell death

To examine the radiosensitizing effects of MEKi in NSCLC cell lines, clonogenic assays were performed to investigate the radiosensitivity of these cell lines under conditions where pERK activity is suppressed by MEK inhibitor. The 3 cell lines were treated with 10 nmol/L MEKi for 1 hour and were then exposed to increasing radiation dosage intervals (0, 2, 4, and 6 Gy). As shown in Fig. 4, treatment with MEKi led to a significant radiosensitization in the H358 cell line (DER = 1.621; $P < 0.001$), compared with the more resistant cell lines: A549 (DER = 1.244; $P < 0.05$) and H460 (DER = 1.263; $P < 0.05$). Exposure of the 3 cell lines to concurrent treatment of MEKi and radiation therapy led to increased cell death compared with either treatment alone. Western blot analyses demonstrated that MEK inhibitor enhanced radiosensitizing effect via activated RB in the sensitive cell line H358, with little effect on the more resistant A549 and H460 cell lines (Supplementary Fig. S5).

The combination of MEK inhibitor and CDK4/6 inhibitor radiosensitize resistant cell lines leading to prolonged DNA damage repair and increased apoptosis

Our previous experiments demonstrated the effectiveness of combination (MEKi and CDKi) drug treatment and MEKi led to a significant radiosensitization in sensitive cell line compared with the more resistant cell lines. So we next performed clonogenic assays on the resistant cell lines A549 and H460. We found that they exhibited a decrease in overall survival fraction when CDK4 inhibitor and MEK inhibitor were coadministered with radiotherapy (Fig. 5A). Combination treatment of MEK inhibitor and

Figure 2.
p16/CDK4/RB regulatory protein status determines cellular sensitivity to MEK inhibitor. A, TCGA provided data on overall survival depending upon p16 status in lung adenocarcinoma tumor samples. Wild-type versus mutant, $n = 230$, $P < 0.05$. B and C, A549 and H460 exhibited decreased cell viability when p16 plasmid vectors were accompanied with increasing concentrations of MEKi (*, $P < 0.05$ compared with the control group). D and E, MTS assays showed that knockdown of CDK4 in p16-deficient cell lines (A549 and H460) increases the effectiveness of GSK1120212 on cell viability. RB depletion restores growth in the presence of MEK inhibitor. F, relative viability of H358 cells treated with 10 or 100 nmol/L GSK1120212 after knockdown of RB. G, Western blot analyses were run 48 hours after transfection with RB siRNA to determine the apoptotic effects with or without GSK1120212.

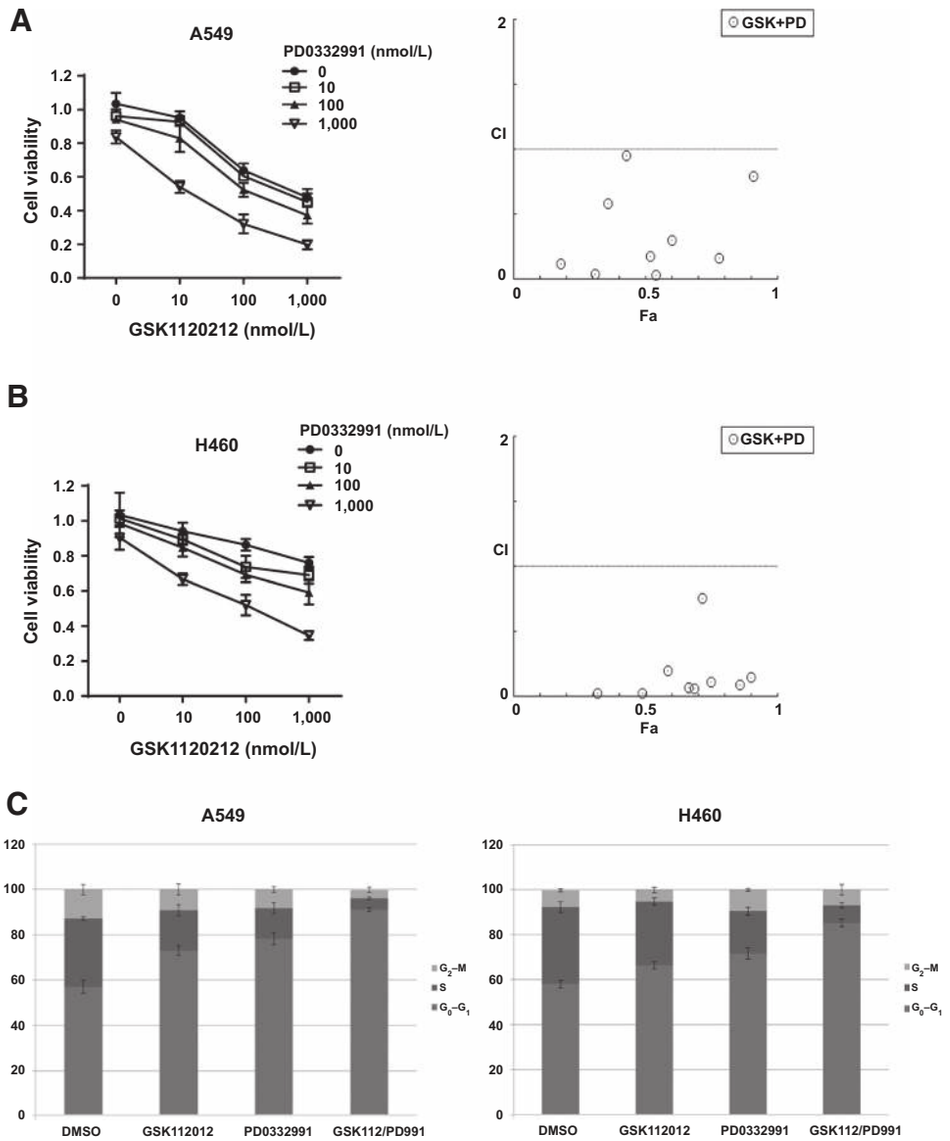

Figure 3.
Coadministration of GSK1120212 and CDK inhibitor (PD0332991) leads to cell-cycle arrest and decreases proliferation through synergistic interaction. A, synergistic interaction between GSK1120212 and PD0332991 in NSCLC cells A549 and H460. Cells were treated with various concentrations of GSK1120212 in combination with PD0332991 for 72 hours, and cell viability was measured by MTS assay. The CI value was determined from the Fa value of each combination according to the Chou–Talalay method by using CompuSyn software (ComboSyn, Inc.), and a CI below 1 represents synergism. B, a cell-cycle analysis was performed on the 2 resistant cell lines to observe the effects on progression of the cell cycle 10 nmol/L GSK1120212 and 1 μmol/L PD0332991.

CDK4/6 inhibitor with radiotherapy in the resistant cell lines increased apoptosis compared with either treatment alone. Both cell lines (A549, H460) were pretreated with 10 nmol/L GSK1120212 and 1 μmol/L PD0332991 for 1 hour. Cells were then treated with or without 6 Gy irradiation, and after 48 hours, the cells were stained with Annexin V and PI for analysis by flow cytometry. The Annexin V/PI data indicated that combination therapy of MEK inhibitor and CDK4/6 inhibitor with radiotherapy led to a significant increase in cell apoptosis rate (Fig. 5B). Western blot analyses performed after 48 hours demonstrated increased levels of apoptosis (e.g. cleaved PARP) when the resistant cell lines were treated with both drugs and radiotherapy compared with either treatment alone (Fig. 5C). One interesting finding was that CDKi and radiotherapy led to equal decreases in pRB compared with both drugs and radiotherapy. The main discovery differentiating this similarity was the respective levels of cleaved PARP (drug combination and radiotherapy had highest levels of apoptosis). This is in line with previous studies that demonstrate MEKi can result in increased levels apoptosis (33). Therefore, this further validated the sensitizing effects that coadministration of these 2 drugs have in resistant cell lines.

Further experiments were carried out on A549 cell line to evaluate the induction and repair of DNA double-strand breaks by counting phosphorylated histone H2AX (γH2AX) foci. The percentage of cells displaying more than 50 foci was determined at 1, 6, and 24 hours after cells were treated with CDK4/6 and MEK inhibitors as in the clonogenic assay and treated with 6-Gy irradiation. Exposure to MEK inhibitor, CDK4/6 inhibitor, or combination group followed by 6 Gy resulted in a number of γH2AX foci not significantly higher than that observed with 6 Gy alone at 1 hour, suggesting that these treatments do not impact immediate DNA damage after radiation. Coadministration of MEK inhibitor and CDK4/6 inhibitor led to an overall increase in the percentage of cells displaying greater than 50 γH2AX foci after 24 hours compared with vehicle or CDK4/6 inhibitor- and radiotherapy-treated cells (Fig. 5D) but not in MEK inhibitor and

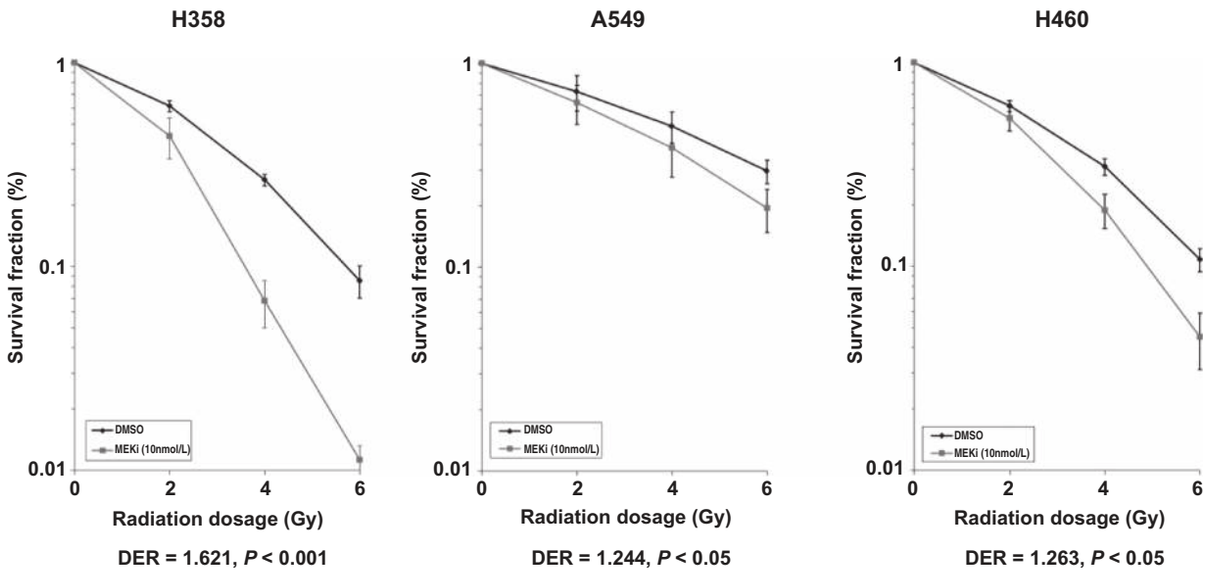

Figure 4.
MEK inhibitor enhances radiosensitivity of KRAS-mutant NSCLC cell lines. A, clonogenic assays were performed on the 3 cell lines (H358, A549, H460) to measure the radiosensitization effects. Cells were treated with 10 nmol/L GSK1120212 or DMSO for 1 hour prior to radiation. Twenty-four hours after irradiation, media were removed and fresh drug-free media were added. Colony-forming efficiency was determined 10 to 12 days later, and survival curves were generated after normalizing for cell killing by drug alone. Values shown represent the mean ± SD of 3 independent experiments. DER for H358 was 1.621 ($P < 0.001$), A549 was 1.244 ($P < 0.05$), and H460 was 1.263 ($P < 0.05$).

radiotherapy group. A second analysis of the damaged DNA foci was performed to create a higher benchmark on effectiveness of treatment. Our data showed that after 24 hours, the combination treatment with radiation had more cells with >100 foci compared with MEKi and radiotherapy ($P < 0.05$), indicating that combination group resulted in inhibition of DNA repair (Fig. 5E).

Combination of MEK inhibitor and CDK4/6 inhibitor sensitizes lung cancer xenografts to radiotherapy

To evaluate whether the enhancement of radiation sensitization observed *in vitro* could be translated into an *in vivo* tumor model, we performed *in vivo* studies on combined drug treatment and radiation therapy. Athymic nude mice bearing A549 tumor xenografts were used for tumor growth delay assay (Fig. 6A). Once a tumor was palpable (~100 mm^3), mice were randomized into vehicle control and treatment groups ($n = 6$/group). We found that, in the absence of radiation, neither MEK inhibitor nor CDK4/6 inhibitor had a significant effect on tumor growth. In combination with fractioned radiation, MEK inhibitor produced significant radiosensitization compared with radiation alone ($P < 0.05$), whereas CDK4/6 inhibitor produced little radiosensitization. Finally, treatment with combination of MEK inhibitor, CDK4/6 inhibitor, and radiation caused no obvious systemic toxicity as assessed by weight loss (Fig. 6B). Histologic sections were also obtained to visualize Ki-67, pERK, and cleaved caspase-3 expression levels in the tumor models. Consistent with our *in vitro* data, decreased levels of phosphorylation of ERK were noted for groups treated with MEK inhibitor (Fig. 6C). In addition, immunostaining of Ki-67 and cleaved caspase-3 revealed diminished proliferation and increased apoptosis within tumors from mice treated with MEK inhibitor in combination with CDK4/6 inhibitor and radiation (Fig. 6D and E). Taken together, these *in vivo* data indicate that MEK inhibitor and CDK4 inhibitor are well-tolerated when coadministered and produce dramatically significant radiosensitization in human lung tumor models.

Discussion

While many treatments have been developed for NSCLCs that have activating mutations in signal transduction pathways, KRAS-mutant NSCLCs have continually led down a path of therapeutic resistance (12–13). Recent findings highlight that KRAS mutations act as a negative predictive marker for tumor response in patients with NSCLCs treated with adjuvant chemotherapy or anti-EGFR therapies (7, 27, 34, 35). An effective therapeutic strategy for KRAS-mutant NSCLC is urgently needed to improve clinical outcomes.

In the present study, we identified resistance of KRAS-mutant NSCLCs to MEK inhibitor in cell lines that harbor CDK2NA mutations. We described a drug combination that was able to sensitize the resistant KRAS-mutant cell lines and also reactivate the RB tumor suppressor pathway leading to increased levels of G_1–G_0 arrest and apoptosis. Previous reports have shown the diversity of KRAS-mutant NSCLCs and the need to look at these cell lines comprehensively to prevent resistance in treatments (36, 37). Approaching signaling pathways in different ways may provide a new opportunity in the treatment and prognosis of KRAS-mutant NSCLCs. It has been suggested that treatments that target intrinsic cancer biology yield opportunities to effectively treat and manage disease (38, 39). The key signal transduction pathways that have been implicated in the pathogenesis of NSCLCs are EGFR, Ras/Raf/Mek/Erk, ALK, and PI3K/Akt (40). Drugs that selectively target these molecules might, therefore, provide therapeutic potential.

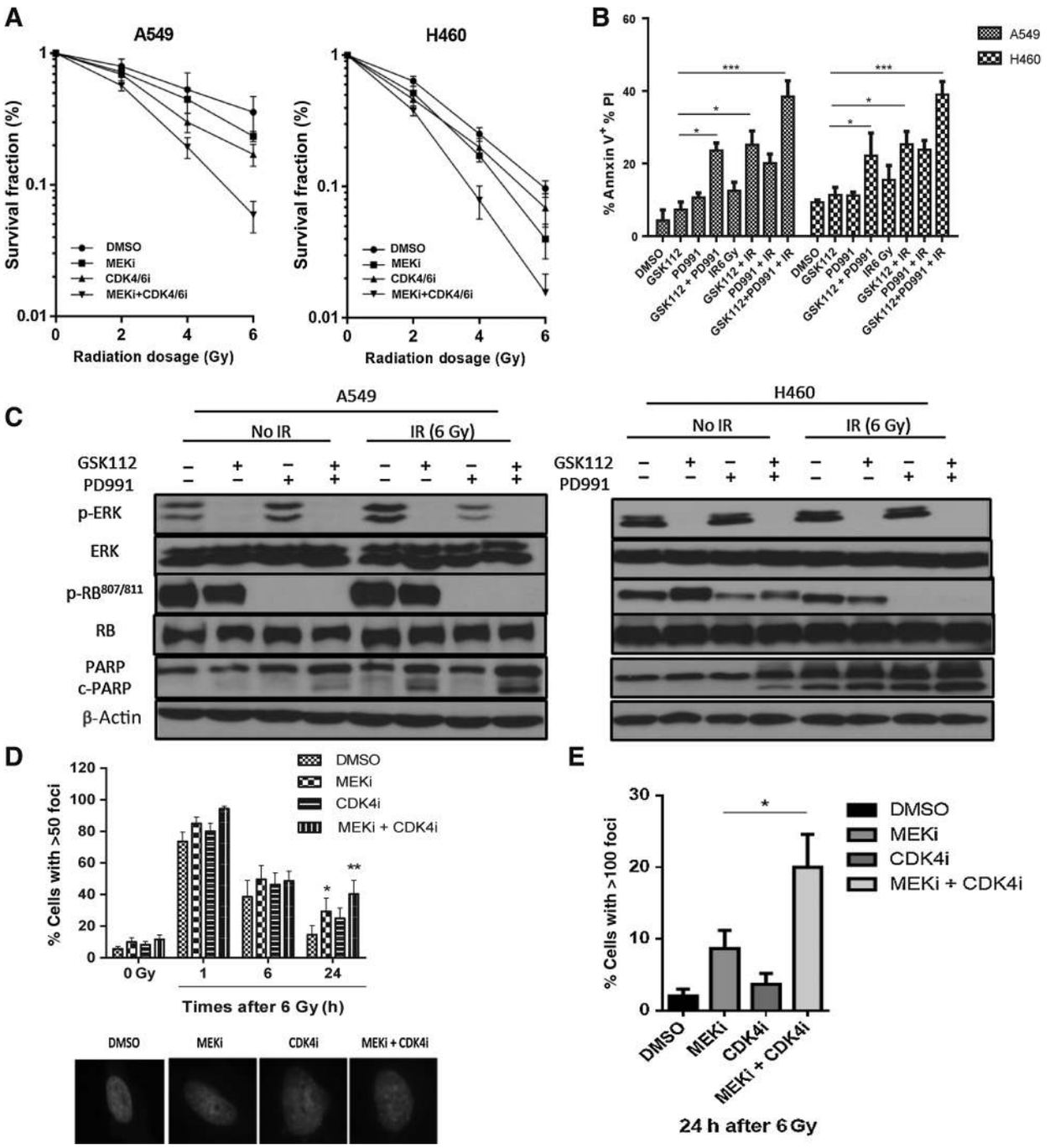

Figure 5.

CDK inhibitor and MEK inhibitor radiosensitize resistant cell lines leading to prolonged DNA damage response and apoptosis. Clonogenic assays (A) were performed on the resistant cell lines A549 and H460 showing the decreased levels of cell survival that coadministration of CDKi and MEKi have when the cells are treated with radiation therapy (0, 2, 4, 6 Gy) compared with either treatment alone. Purple line, control; pink line, MEKi (10 nmol/L); red line, CDK4i (1 μmol/L); and light blue line, MEKi + CDK4i. B, after 48 hours and exposure to 6 Gy, cells were prepared for Annexin V/PI analysis by flow cytometry. Data are represented as mean ± SEM ($n = 3$ independent experiments), where *, $P < 0.05$ and ***, $P < 0.001$ compared with MEKi group. Western blot analyses (C) showed the cells treated with GSK1120212 alone or combined with PD0332991 prior to irradiation with 6 Gy. Immunofluorescent analysis of γH2AX foci was performed on A549 cell line, the percentage of cells displaying >50 foci (D) per cell at the indicated time points and >100 foci (E) per cell at 24 hours after irradiation were determined.

By studying multiple KRAS-mutant NSCLC cell lines, that exhibit different levels of sensitivity and resistance, we were able to determine differences when exposed to MEK inhibitor. MEK1/2 are kinases that connect the RAS/RAF/MEK/ERK proliferative pathway. In their active phosphorylated state, they play a critical role in tumor growth and progression, particularly in KRAS-

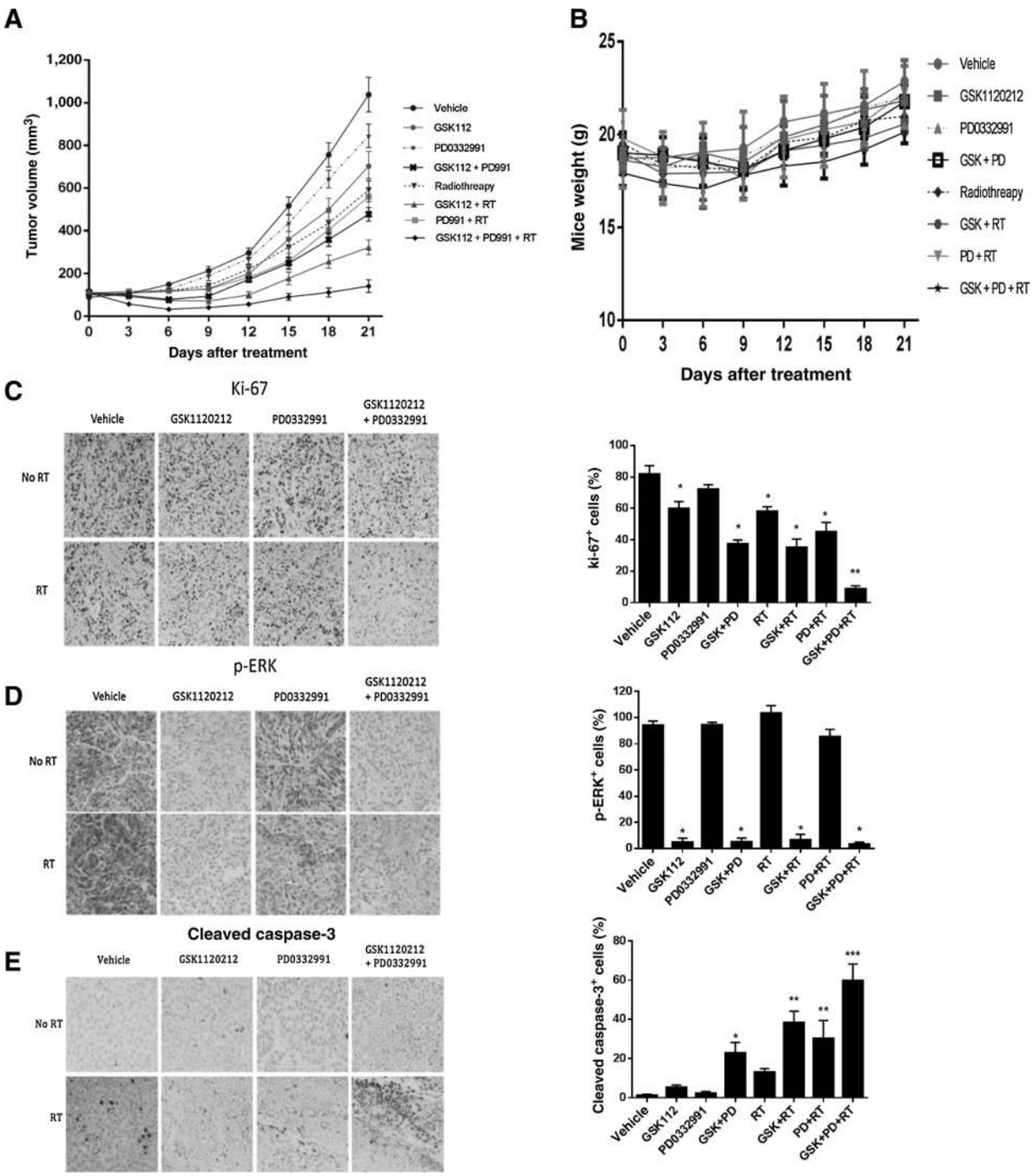

Figure 6.

Combination of MEKi and CDKi sensitizes lung cancer xenografts to radiotherapy. Subcutaneous injections of 2×10^6 A549 cells were performed in athymic nude mice. When A549 tumors reached 100 mm^3 in size, mice were treated with various combinations of MEKi, CDKi, and RT as described in Materials and Methods. Tumor volumes were calculated using the formula: $v = \text{length} \times \text{width} \times \text{width} \times 0.52$. Data, means ± SE; $n = 8$ animals in each group. The 2-sided Student t test was used for comparisons between 2 groups. Statistical significance is designated as: $P < 0.05$ versus vehicle. A, body weights were measured and are expressed as mean ± SD. B, histologic sections were obtained from mice harboring A549 tumors at day 4 after various treatments. Immunohistochemical staining of formalin-fixed, paraffin-embedded tumor tissue for Ki-67 (C), phospho-ERK (D), and cleaved caspase-3 (E). Data for quantified IHC was shown as mean ± SEM for $n = 4$ tumors in each group (E and F). *, $P < 0.05$, **, $P < 0.01$, ***, $P < 0.001$, compared with vehicle.

mutant tumor cells (41). Mutations in KRAS lead to constitutive activation of the RAS pathway, which allows for downstream effectors of ERK1/2 (e.g., cyclin D1, cyclin D1–CDK4 complex) to also be upregulated (42). The MEKi used in this present study is an allosteric inhibitor of MEK1/2 activity preventing the subsequent phosphorylation of ERK1/2 (43). Our study showed that MEKi had the ability to halt cellular growth and survival in KRAS-mutant NSCLCs in a time- and dose-dependent manner. The differences exhibited in cell survival rates with concomitant decreased levels of pERK indicated that this was due to differences in their intrinsic cellular nature. Our data suggested that some of the KRAS-mutant NSCLC cells are intrinsically resistant to MEK inhibition alone. MEKi failed to induce sustained growth arrest and senescence at concentrations that initially block ERK activity as evidenced by decreased ERK phosphorylation.

After performing a TCGA database search, we determined that a mutation in p16 leads to a reduction in overall survival when compared with the wild-type. The data showed that patients with p16 mutation have lower overall survival rate than patients with p16 wild-type (Fig. 2A). Next, we profiled the nature of 6 KRAS-mutant cell lines that harbor different gene mutation and found that cells deficient in p16 exhibited a resistance to the use of MEK inhibitors (Supplementary Fig. S2A and S2B). Because one of the mechanisms of this MEKi is reactivation of RB protein, we decided to test the introduction of p16 plasmids into the cells lacking p16 protein. The introduction of p16 plasmid with concomitant use of MEKi led to the sensitization of previously resistant cell lines compared with either treatment alone (Fig. 2B).

The critical role of RB and p16 status in KRAS-mutant NSCLCs responsiveness to MEK inhibition led us to examine the pharmacologic introduction of synthetic CDK4/6 inhibitors. There is normally a balance between RB proteins binding E2F transcription factors preventing progression of cell cycle and phosphorylation of RB by CDK4/6—cyclin D inhibiting RB–E2F activation. E2Fs regulate transcription of proteins involved in cell-cycle progression, nucleotide biosynthesis, DNA replication, and mitotic progression (44). Studies on glioblastomas have also shown the importance of RB when exposed to CDK4 inhibitors. This study showed that a lack of a functional RB protein when exposed to CDKi led to a decreased effect on cell-cycle arrest and senescence (45). The RB pathway, therefore, represents a critical piece in modulating anticancer treatments (44, 46–48).

Recent advances in clinical studies have identified PD0332991 (e.g., palbociclib) as a potent and highly specific inhibitor of CDK4/6. It has, therefore, been shown to be an effective antiproliferative agent against retinoblastoma (Rb)-positive tumor cells *in vitro*, inducing an exclusive G_1 arrest, with a concomitant reduction of phospho-Ser^{780}/Ser^{795} on the Rb protein (45, 49, 50). Recent studies have also shown that pharmacologic inhibition of MEK triggers modest cell-cycle arrest and radiosensitizes KRAS-mutant NSCLCs to radiation treatment (33). Accordingly, combined pharmacologic inhibition of MEK and CDK4/6 represents an ideal regimen and has been shown to lead to significant synergy *in vivo* in melanoma cells (28). In the case of KRAS-mutant NSCLCs, we showed that silencing (siRNA) and pharmacologic inhibition of CDK4/6 led to a synergistic effect when coadministered with MEKi in resistant cell lines (Fig. 3A). We found no synergism in the sensitive cell line (i.e. H358), which has a functional p16 protein (Fig. 1C and Supplementary Fig. S3). This further validated our conclusions that the addition of a CDKi can resensitize resistant cell lines to MEKi, generating decreased levels of cell viability similar to that in cell lines already sensitive to MEK inhibitor.

The RB pathway is a conglomeration of activating and inhibitory interactions that modulate the progression of the cell cycle (44). Our experiments showed that the use of CDK4/6 inhibitor in conjunction with MEK inhibitor, particularly in cell lines deficient in p16, greatly decreased the cell viability of NSCLCs. Our findings are of clinical relevance because of the sensitization that we demonstrated in KRAS-mutant NSCLCs.

To our knowledge, we showed for the first time that MEK inhibitor and CDK4/6 inhibitor with the addition of radiation could sensitize KRAS-mutant NSCLCs. The coadministration of the 2 inhibitors, plus the addition of radiation therapy, led to a significant increase in cell death and a reduction in overall tumor volume. Here we identify inherent resistance of KRAS-mutant NSCLCs to MEKi due to p16 mutation status and described a drug combination that efficiently reactivates the RB tumor suppressor pathway to trigger radiosensitizing effects, apoptosis, and cell-cycle arrest. The critical role that p16 status has in KRAS-mutant NSCLCs responsiveness to MEK inhibitor shows that this could be used as one of the biomarkers to guide treatment of these patients and improve outcomes. Further studies are required to determine the exact mechanism of sensitization.

Disclosure of Potential Conflicts of Interest

No potential conflicts of interest were disclosed.

Authors' Contributions

Conception and design: Z. Tao, J.M. Le Blanc, Z. Yuan, B. Lu
Development of methodology: Z. Tao
Acquisition of data (provided animals, acquired and managed patients, provided facilities, etc.): Z. Tao, J.M. Le Blanc, P. Wang
Analysis and interpretation of data (e.g., statistical analysis, biostatistics, computational analysis): Z. Tao, J.M. Le Blanc, T. Zhan, B. Lu
Writing, review, and/or revision of the manuscript: Z. Tao, J.M. Le Blanc, H. Zhuang, B. Lu
Administrative, technical, or material support (i.e., reporting or organizing data, constructing databases): Z. Tao, J.M. Le Blanc, C. Wang
Study supervision: Z. Yuan, B. Lu

Received March 13, 2015; revised July 14, 2015; accepted August 3, 2015; published online January 4, 2016.

References

1. Siegel R, Naishadham D, Jemal A. Cancer statistics, 2013. CA Cancer J Clin 2013;63:11–30.
2. Brunelli L, Caiola E, Marabese M, Broggini M, Pastorelli R. "Capturing the metabolomic diversity of KRAS mutants in non-small-cell lung cancer cells. Oncotarget 2014;5:4722–31.
3. Sequist LV, Heist RS, Shaw AT, Fidias P, Rosovsky R, Temel JS, et al. Implementing multiplexed genotyping of non-small-cell lung cancers into routine clinical practice. Ann Oncol 2011;22: 2616–410.
4. Maemondo M, Inoue A, Kobayashi K, Sugawara S, Oizumi S, Isobe H, et al. Gefitinib or chemotherapy for non-small-cell lung cancer with mutated EGFR. N Engl J Med 2010;362:2380–8.
5. Paez JG, Janne PA, Lee JC, Tracy S, Greulich H, Gabriel S, et al. EGFR mutations in lung cancer: correlation with clinical response to gefitinib therapy. Science 2004;304:1497–500.
6. Shaw AT, Kim DW, Nakagawa K, Seto T, Crino L, Ahn MJ, et al. Crizotinib versus chemotherapy in advanced ALK-positive lung cancer. N Engl J Med 2013;368:2385–94.

7. Pao W, Wang TY, Riely GJ, Miller VA, Pan Q, et al. KRAS mutations and primary resistance of lung adenocarcinomas to gefitinib or erlotinib. PLoS Med 2005;2:0057–61.
8. Raponi M, Winkler H, Dracopoli NC. KRAS mutations predict response to EGFR inhibitors. Cur Op Pharm 2008;8:413–8.
9. Shimizu T, Tolcher AW, Papadopoulos KP, Beeram M, Rasco DW, et al. The clinical effect of the dual-targeting strategy involving PI3K/AKT/mTOR and RAS/MEK/ERK pathways in patients with advanced cancer. Clin Cancer Res 2012;18:2316–25.
10. Haura EB, Ricart AD, Larson TG, Stella PJ, Bazhenova L, et al. A phase II study of PD-0325901, an oral MEK inhibitor, in previously treated patients with advanced non-small cell lung cancer. Clin Cancer Res 2010;16:2450–7.
11. Downward J. Targeting RAS signaling pathways in cancer therapy. Nat Rev Cancer 2003;3:11–22.
12. Shaw AT, Winslow MM, Magendantz M, Ouyang C, Dowdle J, Subramanian A, et al. Selective killing of K-ras mutant cancer cells by small molecule inducers of oxidative stress. PNAS 2011;108:8773–8.
13. Watanabe M, Sowa Y, Yogosawa M, Sakai T. Novel MEK inhibitor trametinib and other retinoblastoma gene (RB)-reactivating agents enhance efficacy of 5-fluorouracil on human colon cancer cells. Cancer Sci 2013; 104:687–93.
14. Pylayeva-Gupta Y, Grabocka E, Bar-Sagi D. Ras oncogenes: weaving a tumorigenic web. Nat Rev Cancer 2011;11:761–74.
15. Davies BR, Logie A, McKay JS, Martin P, Steele S, Jenkins R, et al. AZD6244 (ARRY-142886), a potent inhibitor of mitogen-activated protein kinase/extracellular signal-regulated kinase kinase 1/2 kinases: mechanism of action in *vivo*, pharmacokinetic/pharmacodynamic relationship, and potential for combination in preclinical models. Mol Cancer Ther 2007;6:2209–19.
16. Yeh JJ, Routh ED, Rubinas T, Peacock J, Martin TD, Shen XJ , et al. KRAS/BRAF mutation status and ERK1/2 activation as biomarkers for MEK1/2 inhibitor therapy in colorectal cancer. Mol Cancer Ther 2009;8:834–43.
17. Tentler JJ, Nallapareddy S, Tan AC, Spreafico A, Pitts TM, et al. Identification of predictive markers of response to the MEK1/2 inhibitor selumetinib (AZD6244) in K-ras-mutated colorectal cancer. Mol Cancer Ther. 2010; 9:3351–62.
18. Beeram M, Patnaik A, Rowinsky EK. Raf: a strategic target for therapeutic development against cancer. J Clin Oncol 2005;23:6771–90.
19. Sebolt-Leopold JS, Herrera R. Targeting the mitogenactivated protein kinase cascade to treat cancer. Nat Rev Cancer 2004;4:937–47.
20. Young A, Lyons J, Miller AL, Phan VT, Alarcón IR, McCormick F. Ras signaling and therapies. Adv Cancer Res 2009;102:1–17.
21. Adjei AA, Cohen RB, Franklin W, Morris C, Wilson D, Molina JR, et al. Phase I pharmacokinetic and pharmacodynamic study of the oral, small-molecule mitogen-activated protein kinase kinase 1/2 inhibitor AZD6244 (ARRY-142886) in patients with advanced cancers. J Clin Oncol 2008; 26:2139–46.
22. Montagut C, Settleman J. Targeting the RAF-MEK-ERK pathway in cancer therapy. Cancer Lett 2009;283:125–34.
23. Wee S, Jagani Z, Xiang X, Loo A, Dorsch M, Yao Y, et al. PI3K pathway activation mediates resistance to MEK inhibitors in KRAS mutant cancers. Cancer Res 2009;69:4286.
24. Puyol M, Martin A, Dubus P, Mulero F, Pizcueta P, Khan G, et al. A synthetic lethal interaction between K-Ras oncogenes and Cdk4 unveils a therapeutic strategy for non-small cell lung carcinoma. Cancer Cell 2010;18:63–73.
25. Aktas H, Cai H, Cooper GM. Ras links growth factor signaling to the cell cycle machinery via regulation of cyclin D1 and the Cdk inhibitor p27KIP1. Mol Cell Biol 1997;17:3850–7.
26. Gilmartin AG, Bleam MR, Groy A, Moss KG, Minthorn EA, Kulkarni SG, et al. Activation with favorable pharmacokinetic properties for GSK1120212 (JTP-74057) is an inhibitor of MEK activity and sustained in *vivo* pathway inhibition. Clin Cancer Res 2011;17:989–1000.
27. Winton T, Livingston R, Johnson D, Rigas J, Johnston M, et al. Vinorelbine plus cisplatin vs. observation in resected non-small-cell lung cancer. N Engl J Med 2005;25:2589–97.
28. Kwong LN, Costello JC, Liu H, Jiang S, Helms TL, Langsdorf AE, et al. Oncogenic NRAS signaling differentially regulates survival and proliferation in melanoma. Nature Med 2012;18:1503–10.
29. Cancer Genome Atlas Research Network. Comprehensive molecular profiling of lung adenocarcinoma. Nature 2014;511:543–50.
30. Chou TC. Drug combination studies and their synergy quantification using the Chou-Talalay method. Cancer Res 2010;70:440–6.
31. Ohtani N, Yamakoshi K, Takahashi A, Hara E. The p16INK4a-RB pathway: molecular link between cellular senescence and tumor suppression. J Med Invest 2004;51:146–53.
32. Giacinti C, Giordano A. RB and cell cycle progression. Oncogene 2006; 25:5220–7.
33. Lin SH, Zhang J, Giri U, Stephan C, Sobieski M, Zhong L, et al. A high content clonogenic survival drug screen identifies MEK inhibitors as potent radiation sensitizers for KRAS mutant non-small-cell lung cancer. J Thorac Oncol 2014;9:965–73.
34. Massarelli E, Varella-Garcia M, Tang X, Xavier AC, Ozburn NC, et al. KRAS mutation is an important predictor of resistance to therapy with epidermal growth factor receptor tyrosine kinase inhibitors in non-small-cell lung cancer. Clin Cancer Res 2007;13:2890–6.
35. Van Cutsem E, Kohne CH, Hitre E, Zaluski J, Chang Chien CR, et al. Cetuximab and chemotherapy as initial treatment for metastatic colorectal cancer. N Engl J Med 2009;360:1408–17.
36. Okumura S, Janne PA. Molecular pathways: the basis for rational combination using MEK inhibitors in KRAS-mutant cancers. Clin Cancer Res 2014;20:4193–9.
37. Steckel M, Molina-Arcas M, Weigelt B, Marani M, Warne PH, Kuznetsov H, et al. Determination of synthetic lethal interactions in KRAS oncogene-dependent cancer cells reveals novel therapeutic targeting strategies. Cell Res 2012;22:1227–45.
38. Hanahan D, Weinberg RA. The hallmarks of cancer. Cell 2010;100:57–70.
39. Dickson MA. Molecular pathways: CDK4 inhibitors for cancer therapy. Clin Cancer Res 2014;20:3379–83.
40. Heist RS, Engelmen JA. SnapShot: non-small cell lung cancer. Cancer Cell 2012;3:448.
41. Yoshida T, Kakegawa J, Yamaguchi T, Hantani Y, Okajima N, Sakai T. Identification and characterization of a novel chemotype MEK inhibitor able to alter the phosphorylation state of MEK1/2. Oncotarget 2012;3: 1533–45.
42. Zhang X, Cheng Y, Shin J, Kim J, Oh J, Kang J. A CDK4/6 inhibitor enhances cytotoxicity of paclitaxel in lung adenocarcinoma cells harboring mutant KRAS as well as wild-type KRAS. Cancer Bio Ther 2013;14:597–605.
43. Garon EB, Finn RS, Hosmer W, Dering J, Ginther C, Adhami S, et al. Identification of common predictive markers of *in vitro* response to the mek inhibitor selumetinib (AZD6244; ARRY-142886) in human breast cancer and non-small cell lung cancer cell lines. Mol Cancer Ther 2010; 9:1985–94.
44. Knudsen ES, Wang JY. Targeting the RB-pathway in cancer therapy. Clin Cancer Res 2010;16:1094–9.
45. Michaud K, Solomon DA, Oermann E, Kim JS, Zhong WZ, Prados MD, et al. Pharmacologic inhibition of cyclin-dependent kinases 4 and 6 arrests the growth of glioblastoma multiforme intracranial xenografts. Cancer Res 2010;70:3228–38.
46. Roberts PJ, Bisi JE, Strum JC, Combest AJ, Darr DB, Usary JE, et al. Multiple roles of cyclin-dependent kinase 4/6 inhibitors in cancer therapy. J Natl Cancer Inst 2012;104:476–87.
47. Sheppard KE, McArthur GA. The cell-cycle regulator CDK4: an emerging therapeutic target in melanoma. Clin Cancer Res 2013;19:5320–8.
48. Mao CQ, Xiong MH, Liu Y, Shen S, Du XJ, et al. Synthetic Lethal Therapy for KRAS mutant non-small-cell lung carcinoma with nanoparticle-mediated CDK4 siRNA delivery. Mol Ther 2014;22:964–73.
49. Fry DW, Harvey PJ, Keller PR, Elliott WL, Meade M, Trachet E, et al. Specific inhibition of cyclin-dependent kinase 4/6 by PD 0332991 and associated antitumor activity in human tumor xenografts. Mol Cancer Ther 2004; 3:1427–38.
50. Musgrove EA, Caldon CE, Barraclough J, Stone A, Sutherland RL. Cyclin D as a therapeutic target in cancer. Nat Rev Cancer 2011;11:558–72.